Supplementary data

Amorphization of Halide solid electrolyte for Lithium Super-ionic Conductivity

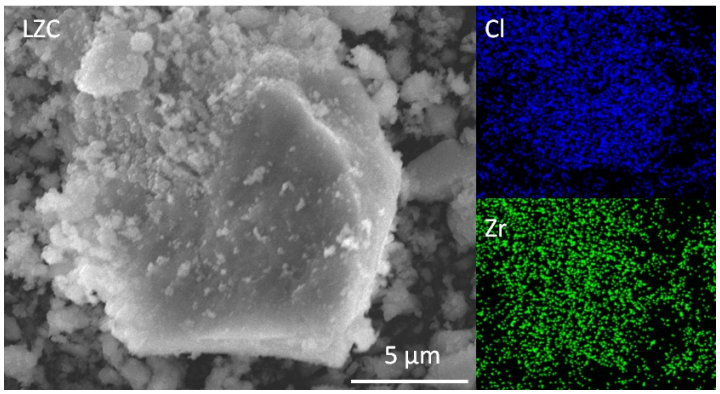

Figure S1. Cross-sectional SEM images and EDS mapping (Cl, Zr) of LZC.

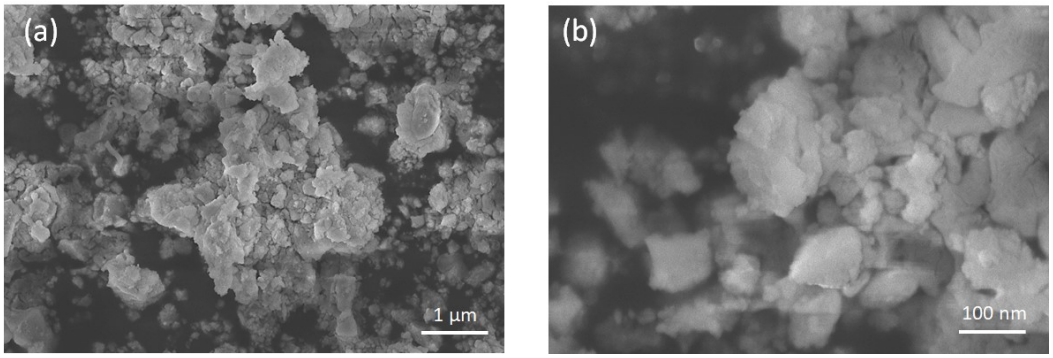

Figure S2. (a) 10Kx and (b) 50Kx SEM images of LZC powder.

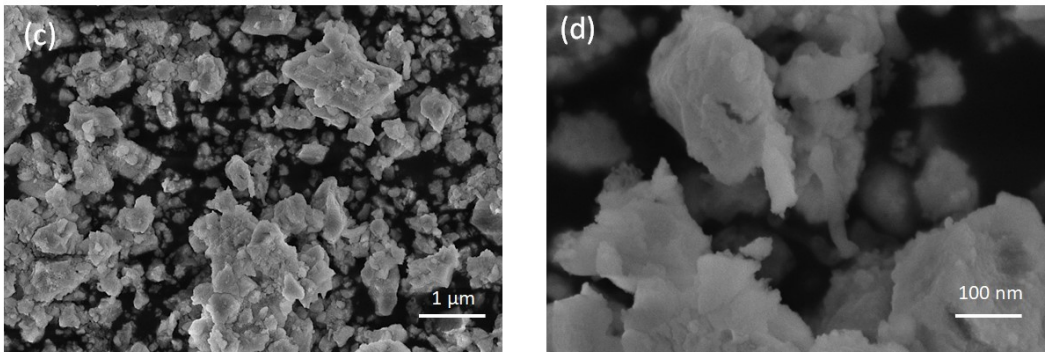

Figure S3. (a) 10Kx and (b) 50Kx SEM images of nc-$LZCS_{0.2}$ powder.

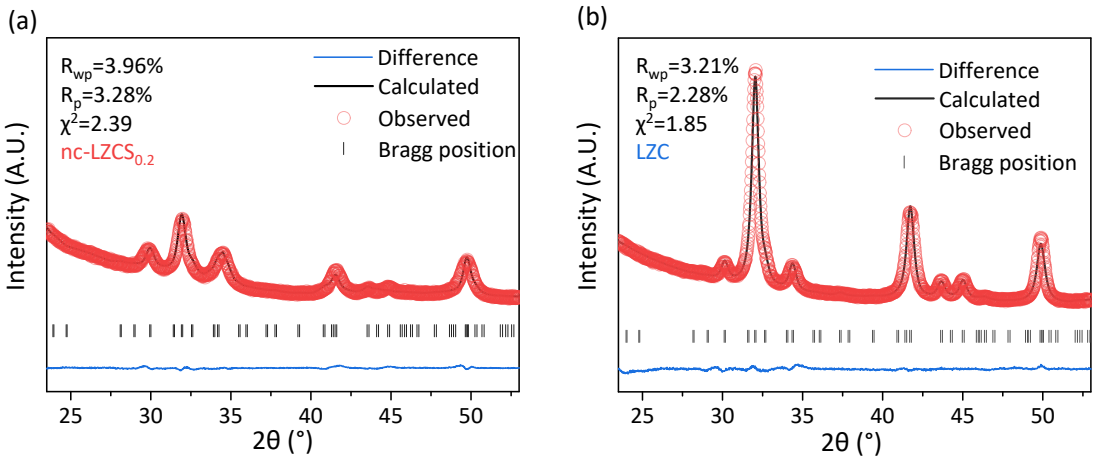

Figure S4. Rietveld refinement of the XRD patterns recorded for as-milled nc-LZCS$_{0.2}$ and LZC, respectively

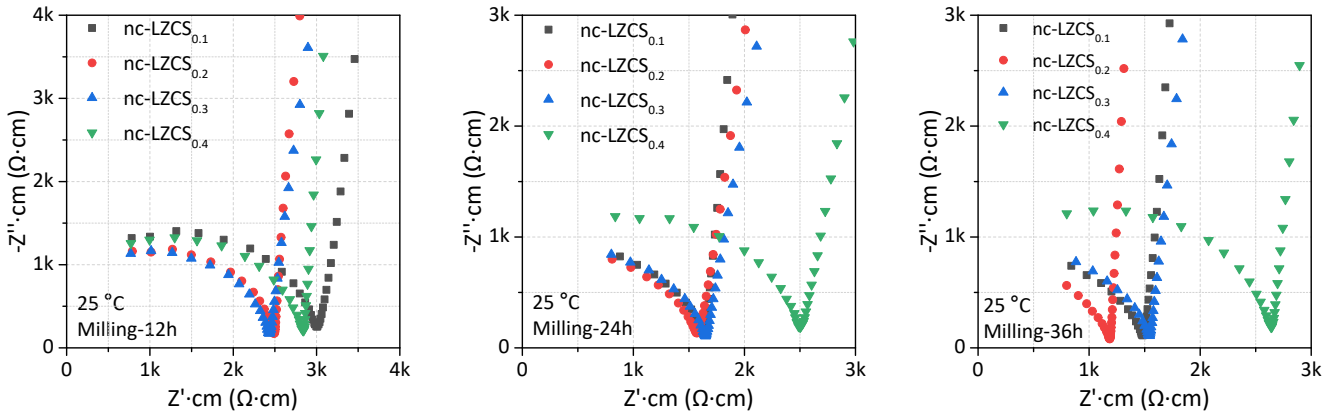

Figure S5. Nyquist plots of nc-LZCS$_x$ for different ball milling times at 25 °C.

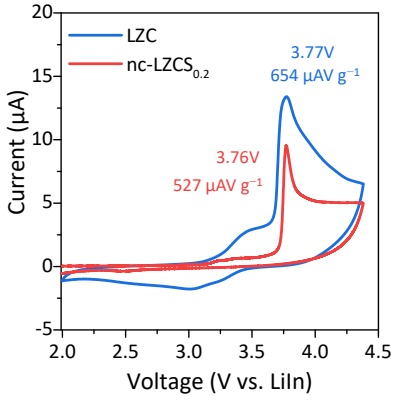

Figure S6. CV curve of LZC and nc-LZCS$_{0.2}$.

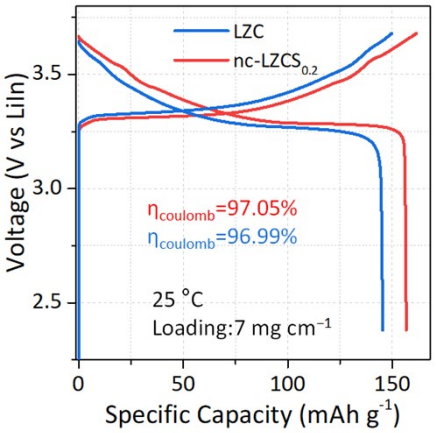

Figure S7. Initial charge/discharge curves obtained at 0.1C for LCO electrodes using nc-$LZCS_{0.2}$ and LZC, with the Coulombic efficiency

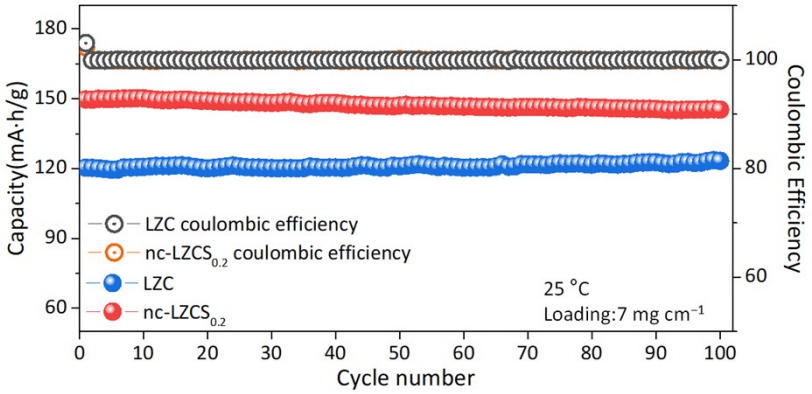

Figure S8. The long-term cycling performance of ASSLB Li-In/LPSC-LZC/LCO and Li-In/LPSC-nc-$LZCS_{0.2}$/LCO cells at 0.3C.

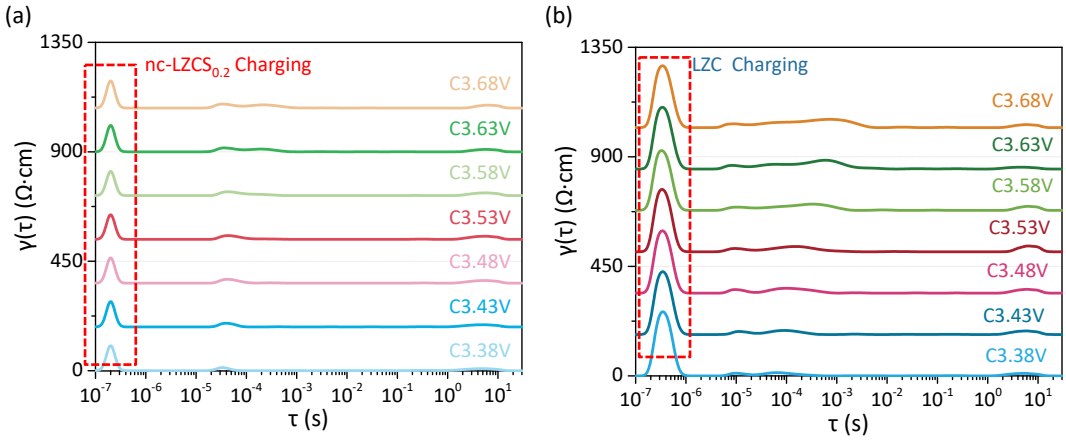

Figure S9. The DRT evolution of ASSLB using nc-$LZCS_{0.2}$ and LZC during first cycle at a 0.1C rate. (a) nc-$LZCS_{0.2}$ charging, (b) LZC charging.

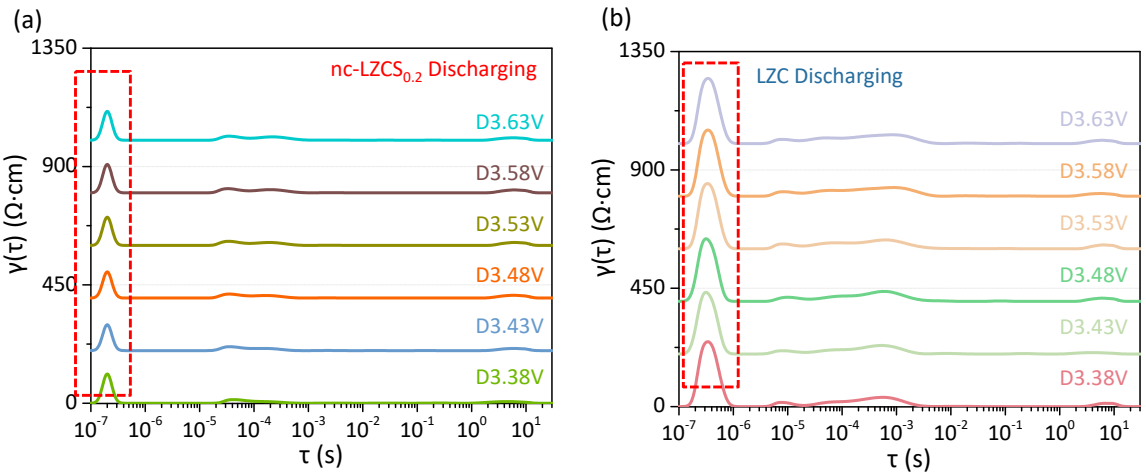

Figure S10. The DRT evolution of ASSLB using nc-LZCS$_{0.2}$ and LZC during first cycle at a 0.1C rate. (a) nc-LZCS$_{0.2}$ discharging, (b) LZC discharging.

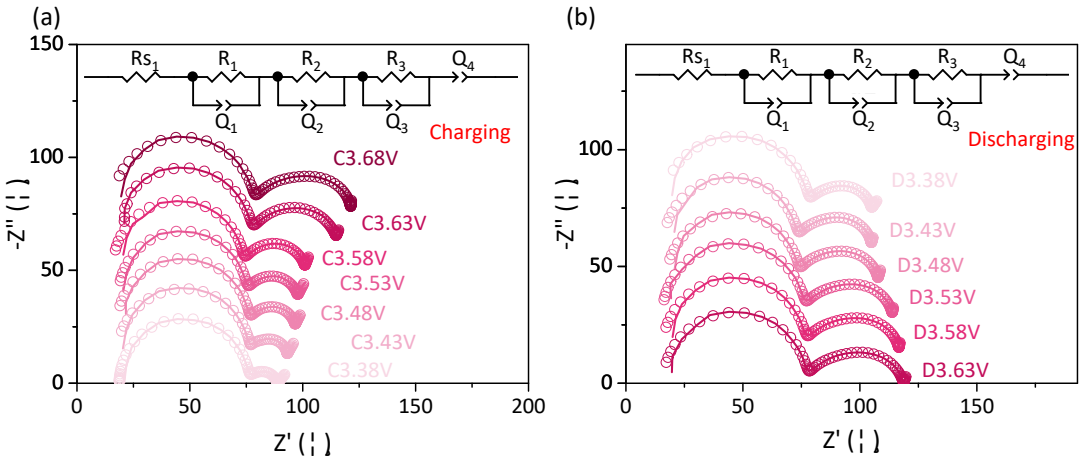

Figure S11. The EIS of ASSLB using nc-LZCS0.2 at charging and discharging process with the used equivalent circuit model as the inset, (a) charging process, (b) discharging process.

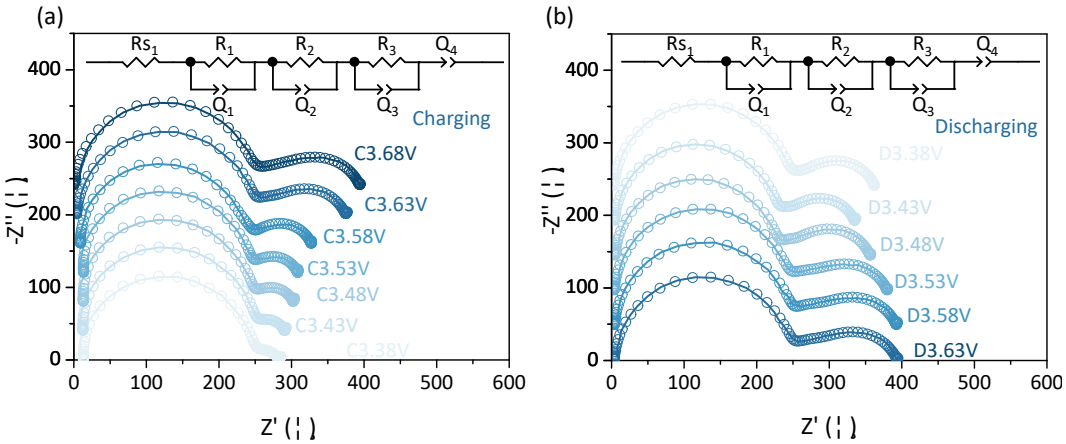

Figure S12. The EIS of ASSLB using LZC at charging and discharging process with the used equivalent circuit model as the inset, (a) charging process, (b) discharging process.

Table S1. The refined lattice parameter values obtained from the XRD pattern of nc-$LZCS_{0.2}$

Atom	Wyckoff site	x	y	z	Occupancy	B_{iso} (Å^2)
Li1	6g	0.28256	0	0	0.21500	0.04525
Li2	6h	0.35830	0	0.5	0.85251	0.03530
Zr1	1a	0	0	0	0.66626	0.01528
Zr2	2d	0.33333	0.66667	0.50549	0.54895	0.00858
Zr3	1b	0	0	0.5	0.45448	0.00545
Zr4	2d	0.33333	0.66667	0.98065	0.39149	0.00514
Cl1	6i	0.10755	-0.10755	0.76565	0.93400	0.01552
Cl2	6i	0.22886	-0.22886	0.25805	0.90553	0.02559
Cl3	6i	0.45418	-0.45418	0.78802	0.91560	0.01560
S1	6i	0.10755	-0.10755	0.76565	0.06600	0.00828
S2	6i	0.22886	-0.22886	0.25805	0.09447	0.00579
S3	6i	0.45418	-0.45418	0.78802	0.08440	0.00158
a = 10.94428 Å			b = 10.94428 Å	c = 5.92621 Å		Vol = 598.058 Å
Space group $P_{\bar{3}m1}$		χ^2= 2.39	R_{wp}= 3.96%	R_p= 3.28%	α = β = 90°	γ = 120°

Table S2. The refined lattice parameter values obtained from the XRD pattern of LZC.

Atom	Wyckoff site	x	y	z	Occupancy	B_{iso} (Å^2)
Li1	6g	0.55957	0	0	0.6357	0.35894
Li2	6h	0.34962	0	0.5	0.38752	0.34581
Zr1	1a	0	0	0	0.59758	0.00251
Zr2	2d	0.33333	0.66667	0.51022	0.54860	0.00381
Zr3	1b	0	0	0.5	0.57245	0.00185
Zr4	2d	0.33333	0.66667	0.96945	0.36955	0.00035
Cl1	6i	0.10938	-0.10938	0.77516	0.99995	0.01585
Cl2	6i	0.22045	-0.22045	0.24275	0.99998	0.04582
Cl3	6i	0.45855	-0.45855	0.68545	0.99980	0.01556
a = 10.97022 Å			b = 10.97022 Å	c = 5.85746 Å		Vol = 618.690 Å
Space group $P_{\bar{3}m1}$		χ^2= 1.85	R_{wp}= 3.21%	R_p= 2.28 %	α = β = 90°	γ = 120º

Table S3. Fitting parameters of ASSLB using nc-$LZCS_{0.2}$ at charging and discharging process.

Sample	Rs1	R1	CPE1-T	CPE2-P	R2	CPE2-T	CPE2-P	R3	CPE3-T	CPE3-P	CPE4-T	CPE4-P
nc-$LZCS_{0.2}$-C3.38V	76.9	13.2	1.583E-9	0.9893	18.2	3.857E-6	0.6258	25.76	2.559E-5	0.5456	0.6487	0.4649
nc-$LZCS_{0.2}$-C3.43V	76.9	12.1	1.734E-9	0.9527	18.44	5.254E-6	0.4291	31.47	6.985E-5	0.2223	0.5648	0.2552
nc-$LZCS_{0.2}$-C3.48V	77.0	28.6	1.934E-9	0.9928	16.51	6.856E-6	0.2477	18.22	4.894E-5	0.9662	0.2255	0.3424
nc-$LZCS_{0.2}$-C3.53V	76.0	14.5	1.324E-9	0.9827	11.31	8.485E-6	0.2862	56.73	2.575E-4	0.8857	0.3116	0.2633
nc-$LZCS_{0.2}$-C3.58V	74.6	23.7	2.896E-9	0.8768	18.31	8.482E-6	0.7348	33.64	8.443E-5	0.5975	0.6237	0.3822
nc-$LZCS_{0.2}$-C3.63V	77.8	11.5	2.236E-9	0.9725	20.2	5.527E-6	0.3248	25.87	9.352E-5	0.2436	0.1323	0.1253
nc-$LZCS_{0.2}$-C3.68V	79.0	14.3	2.863E-9	0.9786	18.2	8.933E-5	0.8782	45.48	6.231E-5	0.3556	0.1782	0.2146
nc-$LZCS_{0.2}$-D3.63V	78.4	26.9	1.824E-9	0.9254	16.66	1.944E-5	0.9127	54.93	7.388E-5	0.5218	0.1546	0.2668
nc-$LZCS_{0.2}$-D3.58V	77.4	22.4	1.833E-9	0.8975	18.19	4.764E-5	0.7157	45.61	2.847E-4	0.4699	0.1627	0.4564
nc-$LZCS_{0.2}$-D3.53V	76.9	14.5	1.724E-9	0.9278	11.75	6.224E-6	0.8624	14.40	4.954E-5	0.6756	0.3919	0.4242
nc-$LZCS_{0.2}$-D3.48V	74.4	22.6	1.862E-9	0.9862	17.98	8.580E-5	0.4827	56.53	6.482E-5	0.7847	0.2494	0.2323
nc-$LZCS_{0.2}$-D3.43V	73.9	23.6	1.719E-9	0.9785	19.52	3.857E-5	0.7815	22.87	6.555E-5	0.6654	0.6558	0.3232
nc-$LZCS_{0.2}$-D3.38V	79.1	10.5	1.715E-9	0.9938	25.85	4.563E-6	0.7895	34.89	4.336E-4	0.5466	0.5279	0.1382

Table S4. Fitting parameters of ASSLB using LZC at charging and discharging process

Sample	Rs1	R1	CPE1-T	CPE2-P	R2	CPE2-T	CPE2-P	R3	CPE3-T	CPE3-P	CPE4-T	CPE4-P
LZC-C3.38V	252.4	17.82	1.691E-9	0.9451	21.28	2.413E-5	0.4434	12.67	2.444E-5	0.3979	0.8896	0.1313
LZC-C3.48V	253.3	25.53	2.653E-9	0.9312	35.58	8.241E-5	0.4292	43.59	4.922E-5	0.6454	0.5442	0.5464
LZC-C3.53V	253.0	35.78	2.314E-9	0.9763	55.81	6.044E-6	0.7864	21.29	5.734E-4	0.7531	0.6824	0.4575
LZC-C3.58V	244.9	38.24	1.229E-9	0.9884	69.79	7.442E-6	0.5722	45.33	9.896E-5	0.9410	0.8938	0.1742
LZC-C3.63V	258.4	42.95	3.412E-9	0.9647	84.42	3.838E-6	0.9533	26.45	7.429E-5	0.2666	0.9249	0.3653
LZC-C3.68V	258.6	87.11	6.103E-9	0.8239	82.20	3.653E-5	0.4376	37.16	5.637E-5	0.4786	0.7260	0.5327
LZC-D3.63V	257.9	68.67	1.357E-9	0.9954	79.61	1.501E-5	0.6252	79.31	3.425E-5	0.9808	0.4584	0.6738
LZC-D3.58V	256.7	35.95	2.845E-9	0.9192	57.84	6.467E-6	0.7433	65.52	8.514E-5	0.2907	0.5105	0.8823
LZC-D3.53V	251.9	21.10	1.630E-9	0.9273	52.95	4.325E-5	0.8943	44.39	1.773E-4	0.3843	0.3242	0.4642
LZC-D3.48V	240.0	22.34	1.284E-9	0.9555	47.44	3.262E-5	0.7895	23.69	2.682E-4	0.2568	0.2353	0.5543
LZC-D3.43V	240.5	15.38	1.053E-9	0.8668	35.25	2.863E-5	0.6654	34.56	4.666E-5	0.5254	0.3265	0.5665
LZC-D3.38V	256.9	13.90	1.669E-9	0.9716	39.73	7.687E-5	0.7469	49.78	3.966E-5	0.8152	0.4321	0.4027